Anisotropy Measurements of Solvated HgI_2 Dissociation: Transition State and Fragment Rotational Dynamics

M. Volk, S. Gnanakaran, E. Gooding, Y. Kholodenko, N. Pugliano, and R. M. Hochstrasser*

Department of Chemistry, The University of Pennsylvania, Philadelphia, Pennsylvania 19104

Received: July 8, 1996; In Final Form: September 30, 1996[⊗]

Pump−probe anisotropy measurements of HgI_2 photodissociation in ethanol were carried out. The reactive motion from electronically excited HgI_2 toward HgI and I is clearly evident in the signal. The subsequent randomization of the HgI orientational distribution occurs in the biphasic manner typical for some other diatomic molecules, with a 500-fs component that has an inertial motion contribution and a slow (8−10-ps) diffusive component. Interpretations of these regions were assisted by molecular dynamics simulations, which also were used to show that the rotational energy relaxation would be very fast in this system. The magnitudes of the anisotropies at different pump wavelengths show that the near-UV absorption of HgI_2 involves overlapping $^1\Sigma^+ \rightarrow {}^1\Sigma^-$ and $^1\Sigma^+ \rightarrow {}^1\Pi$ transitions, consistent with magnetic circular dichroism (MCD) measurements. The anisotropy decay shows oscillations which are proposed to arise from oscillations in the volume and moment of inertia as the vibrational wavepacket moves in the anharmonic HgI potential.

Introduction

The information acquired by time-resolved spectroscopy regarding the dynamics of chemical reactions in solution can be significantly extended by carrying out the experiments in polarized light. Such experiments yield the pump/probe anisotropy which is proportional to the difference between the signal obtained with pump and probe pulses polarized parallel and perpendicular to one another. It permits the determination of the symmetry characteristics of transitions which in turn helps to establish the nature of the electronic states involved in the reaction. It also can enable the detection of coherence and the measurement of coherence loss.[1] The rotations of the transition dipoles, the reactant, the transition states, and the products of the reaction can also be determined.[2] In addition, the anisotropy can help unravel the complex kinetic behavior that can arise from overlapping signals of different species that are rotating and are involved in a reaction.[3,4] In the solution phase, anisotropy measurements have enabled the study of excited-state energy transfer between identical chromophores,[5,6] the dynamics and energy transfer within proteins,[7] the alignment of reactant and product states,[4] and the angular effects of the coupling of internal and overall motions of molecules.[4,8] In the present work, anisotropy measurements are applied to the impulsive photochemical dissociation of HgI_2 which generates iodine atoms and HgI molecules.

The impulsive photolysis of HgI_2 was studied in the gas phase[9−14] and more recently in solutions.[15−17] The excitation of linear HgI_2 by a polarized light pulse occurs via transition moments that are either parallel or perpendicular to the bond axis. The ground state of HgI_2 is of the $^1\Sigma$ type,[18] and the lowest energy absorption band in solution consists of transitions to both $^1\Sigma$ and $^1\Pi$ states.[19] The photoreaction leads to the (X) $^2\Sigma$ state of HgI and both ground and excited states of the I atom.[20] In solution, the reactive motion takes about 90 fs, which corresponds to just less than one-half of a vibrational period. As the molecule dissociates, the electronic wave functions change, and this could be seen in the anisotropy if there were a rotation of the transition moment in the molecular frame. The anisotropy is also sensitive to the presence of electronic coherence introduced by the excitation of degenerate Π states or superpositions of Π and Σ states.[1,21] While the products of the reaction, HgI and I, are forming, their transitions can be probed. This experiment yields information regarding the alignment of the transition moments of the product and the reactant molecules. Any misalignments might arise either from torques associated with the reactive motion or from the coupling of the internal and external motion or from the equilibrium inertial angular motion of HgI modified by the fluctuating torques exerted by the solvent molecules. These fluctuating torques give rise to the rotational diffusion of HgI. However, the effective rotational temperature of reaction products may be time dependent due to the solvent-collision-induced cooling of the initial distribution of states.

The rotational dynamics of diatomic molecules in solutions has been studied theoretically and experimentally.[22] The experiments were mainly carried out in the frequency domain by means of dynamic light scattering, polarized Raman line shapes, or magnetic resonance.[23−29] Recently, a time domain experiment on I_2^- has been reported.[30,31] The characteristic time constant, τ_c, for loss of rotational coherence from an ensemble of rotors at temperature T is given by $(2\pi/9)(I/k_BT)^{1/2}$, where I is the moment of inertia. For HgI at 300 K, the value of τ_c is 1.05 ps. The line shapes of polarized Raman transitions of diatomic molecules frequently indicate that this inertial-like component contributes significantly to the decay of the anisotropy.[32−34] It is usually followed by a slower diffusive component.[35] Several models have been proposed to describe the anisotropy decay for systems which evolve from free rotation at short times to rotational diffusion at long times.[24,34,36−44]

It follows that the anisotropy can be used to examine the angular motion as the nuclei move through the transition state and the rotational energy distribution of a reaction, if the time resolution is faster than rotational energy relaxation. The interpretation of such experiments can be greatly aided by simulations of the classical dynamics. Equilibrium molecular dynamics simulations can help to generate a microscopic interpretation of the experimental measurements of the rotational dynamics. Both the relevant orientational correlation function, $\langle P_2(\cos\theta)\rangle$, where θ is the angle between the pumped and probed dipoles, and the rotational energy correlation function,

[⊗] Abstract published in *Advance ACS Abstracts,* December 15, 1996.

S1089-5639(96)02013-0 CCC: $14.00

TABLE 1: 'Canonical' Values $r_{kj}(0)$ of the Anisotropies Expected for Different Combinations of Pump and Probe Transitions of HgI_2 and HgI

pumped HgI_2 trans	probing HgI_2 trans	probing HgI_2 anisot	probing HgI trans	probing HgI anisot
$\Sigma_g^+ \rightarrow \Pi_u$	$\Pi_u \rightarrow \Sigma_g^+$	0.4	$\Sigma \rightarrow \Sigma$	−0.2
	$\Pi_u \rightarrow \Pi_g$	−0.2	$\Sigma \rightarrow \Pi$	0.1
$\Sigma_g^+ \rightarrow \Sigma_u^-$	$\Sigma_u^- \rightarrow \Sigma_g^+$	0.4	$\Sigma \rightarrow \Sigma$	0.4
	$\Sigma_u^- \rightarrow \Pi_g$	−0.2	$\Sigma \rightarrow \Pi$	−0.2

$\langle \delta E(0) \delta E(t) \rangle$, can be calculated by standard methods from classical trajectories[45,46] and have been reported for a number of diatomic molecules.[24,47−51] Interesting theoretical questions remain concerning the relationship between these two quantities. As yet, there are no direct measurements of rotational energy relaxation in liquids to the best of our knowledge. In the present work, we combine equilibrium simulations of the reactive, inertial-like, and diffusive rotational dynamics with the results of measurements of the photodissociation HgI_2 in ethanol and methanol solutions.

Expectations for the Anisotropy during the HgI_2 Photodissociation

The various possible excited-state assignments for HgI_2 and HgI lead to different anisotropic signals. In principle, these signals can be used to determine the electronic symmetry of the species associated with different positions on the reaction coordinate. The anisotropy that is measured in the experiment, $r_e(t)$, is a time-ordered, nested convolution of the pump and probe electric fields that generate the signal, with the molecular responses that are involved in each of the excitation steps. The *anisotropy response*, $r(t)$, is the anisotropy that would be obtained with δ-function field pulses. In ultrafast experiments, the anisotropy response must be calculated by deconvolution of each of the time-ordered fields involved in generating the signals. However, if the electronic dephasing is fast compared with the measurement time, the parallel and perpendicular signals can be deconvoluted from the pump/probe laser intensity correlation function to yield the impact signals $S_\perp(t)$ and $S_\parallel(t)$, respectively. In the case where observations are made only in spectral regions where new absorptions are created, the anisotropy response is given by

$$r(t) = 0.4 \sum_{j,k} N_k(t) \langle P_2[\mu^j_{\text{pump}}(0) \cdot \mu^k_{\text{probe}}(t)] \rangle = 0.4 \sum_{j,k} N_k(t)\, r_{kj}(t) = \{S_\parallel(t) - S_\perp(t)\}/\{S_\parallel(t) + 2S_\perp(t)\} \quad (1)$$

where the sum is over all transitions from the ground state to excited state j and over all transitions from state k and $\langle \cdots \rangle$ is the ensemble average. N_k is the fraction of the signal from state k at time t, P_2 is the second Legendre polynomial, and the μ's are the pump or probe dipoles associated with these transitions. In what follows, the expectations for the anisotropies that would arise for various states k,j are discussed in terms of the "canonical" values $r_{kj}(0)$ that are given in Table 1.

It is first supposed that the pumped transition is of the $^1\Sigma^+ \rightarrow {}^1\Sigma^-$ type. In this case, before motion away from the transition-state region, the probed transition may be either $^1\Sigma^- \rightarrow {}^1\Sigma^+$ or $^1\Sigma^- \rightarrow {}^1\Pi$, for which the canonical anisotropies would be 0.4 or −0.2, respectively. After dissociation, when the $^2\Sigma \rightarrow {}^2\Sigma$ transition of HgI is probed,[15−17] the canonical anisotropy should become 0.4. The situation is different if the pumped transition is of the $^1\Sigma^+ \rightarrow {}^1\Pi$ type. In that case, probing $^1\Pi \rightarrow {}_1\Sigma^+$ or $^1\Pi \rightarrow {}^1\Pi$ transitions from the transition-state region would yield canonical anisotropies of 0.4 or −0.2, respectively, whereas probing the $^2\Sigma \rightarrow {}^2\Sigma$ transition of HgI would result in a canonical anisotropy of −0.2. Other less likely possibilities for probing transitions of HgI are also given in Table 1. Since HgI_2 has overlapping transitions of the $^1\Sigma^+ \rightarrow {}^1\Sigma^-$ and $^1\Sigma^+ \rightarrow {}_1\Pi$ type in the wavelength region used for excitation in this work,[19] appropriate combinations of these results are expected as described by eq 1. These results assume, as does eq 1, that the electronic coherence has already dephased; otherwise, the anisotropy would be 0.7 for the case where the $^1\Pi \rightarrow {}^1\Sigma$ transition of HgI_2 is probed, as discussed previously.[1,21]

The conclusions reached through Table 1 are subject to the assumption that the solution-phase states of the reactant and the product are of the Π and Σ type. Actually, the Π states must be split by asymmetric solvent interactions. If the static part of this splitting were to become large enough, the excitation pulse might access mostly one component of the perturbed Π state. This would modify the numbers in Table 1.

Experimental Methods

Two different femtosecond laser systems were used in order to investigate the time and excitation wavelength dependence of the anisotropy. One system was based on a regeneratively amplified titanium sapphire laser in which a portion of the fundamental (810 nm) was tripled to obtain a 140-fs pulse at 270 nm. The laser design was based on that described earlier.[52] The other system was a Nd:Yag-amplified CPM laser which was also described previously.[15] With this system, the pump was a 40-fs pulse at 320 nm. The pump intensities were adjusted to be far from saturation; typically less than 1 μJ of pump energy was used. For each experiment, the probe light was obtained from a continuum generated in water. Selection of probe wavelengths (440−560 nm) was accomplished by 10-nm bandpass interference filters. The polarization of the probe light was adjusted to be at an angle of 45° with respect to the polarization of the pump light. After the sample, the probe light was split into two components with a polarizer. These were detected separately so that transient absorption signals for parallel and perpendicular polarization of pump and probe light could be observed simultaneously. This procedure ensures that the two signals are synchronous to an accuracy determined by the pump-induced birefringence in the sample, which is negligible.

The samples consisted of flowing jets of 2−15 mM ethanol solutions of HgI_2 (Aldrich 99.999%, used as received), corresponding to an optical density of 1 at the employed pump wavelength. Time zero was determined with an accuracy of ±15 fs by means of pump/probe experiments on *trans*-stilbene samples. These stilbene samples also served to check the polarization characteristics of the apparatus. The expected anisotropy of 0.4 was reproduced (±0.04) for the 320-nm pump experiments, whereas for 270-nm pump experiments, an anisotropy of 0.32 was observed due to overlapping absorption bands in stilbene at this wavelength. A small, but well-reproducible transient absorbance spike around time zero with an anisotropy of 0.4 was found when pumping pure ethanol at 270 nm. This signal arises from two-photon absorption and was corrected for in the results shown here, although it did not significantly affect the anisotropies observed in the presence of HgI_2.

Experimental Results and Fits

The time-dependent anisotropies $r_e(t)$ of the transient absorption observed after excitation of HgI_2 at 270 and 320 nm are shown in Figure 1 for representative probe wavelengths. Also shown are the transient absorption signals for parallel and perpendicular polarizations of pump and probe light for 270-nm pump, 490-nm probe. As has been discussed explicitly

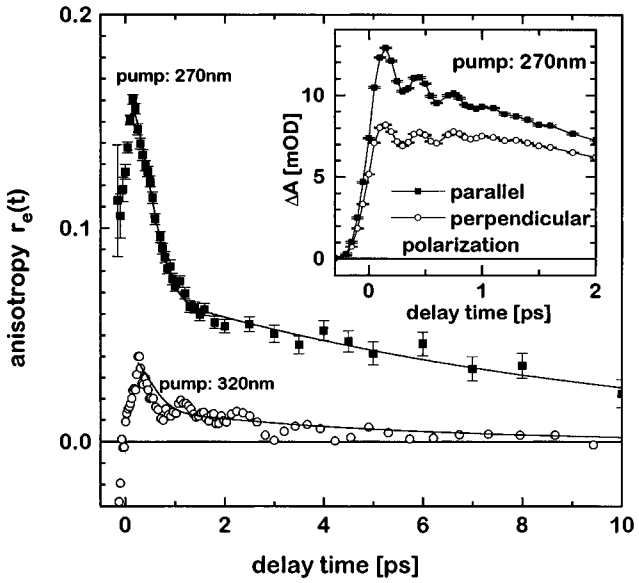

Figure 1. Anisotropies $r_e(t)$ of the transient absorption observed after HgI_2 photolysis for 270-nm pump, 490-nm probe (■) and for 320-nm pump, 440-nm probe (○). Due to the smaller anisotropy observed with 320-nm excitation, these data are noisier. The solid lines correspond to the best fit of the anisotropy decay after 150 fs to a sum of a Gaussian and an exponential, as described in the text. The inset shows the transient absorption signals at 490 nm after excitation at 270 nm observed with parallel and perpendicular polarizations of pump and probe.

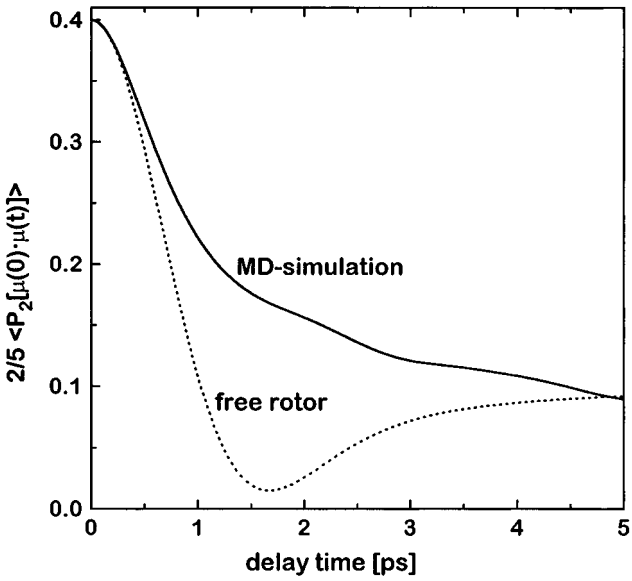

Figure 2. Anisotropy decay $2/5\langle P_2[\mu(0)\cdot\mu(t)]\rangle$ from an equilibrium MD simulation of HgI in ethanol. The dotted line shows the free rotor decay for HgI.

before,[15−17] the initial transient absorption of HgI_2 in the transition-state region is followed by the absorption of the impulsively generated HgI, exhibiting wavepacket motion and vibrational cooling. Although the transient absorption itself depends on the probe wavelength,[15−17] the resulting anisotropy is independent of the probe wavelength in the range 405−560 nm (results not shown). However, $r_e(t)$ shows a significant variation with the pump wavelength.

At the earliest times, the anisotropy is seen to exhibit a sub-100-fs rise to a maximum from a small value. This was more pronounced in the results for 320-nm excitation, which did show a negative anisotropy at early times, than in those for 270-nm excitation (Figure 1), probably because of their better time resolution. The rise occurs during the reactive period while the HgI and I fragments are separating.[15] This period is completed at approximately the time when the first maximum in the oscillatory signal occurs, which corresponds to HgI having reached its most extended configuration for the first time.[15] A quantitative fit of the anisotropy rise time, even assuming the dephased form given in eq 1, requires knowledge of the absorption coefficients of the species present during the reactive motion that are contributing to the signal at the probe wavelength. When assuming equal absorption coefficients of HgI_2 in the transition state and HgI, the decay time of the HgI_2 signal is found to be approximately 65 fs. If the absorption coefficients for HgI were considerably bigger than that of HgI_2, the fit would yield a larger time constant. Besides this uncertainty due to the extinction coefficients, the exact determination of the time constant is hindered by the uncertainty of the initial anisotropy value as well as by the limited time resolution.

After the maximum in the anisotropy, the signal shape is not influenced by the reactive motion or the pulse shapes. It corresponds to a biphasic decay toward zero. In order to extract an initial anisotropy, free from the effects of the reactive part and concerned only with the rotational dynamics of HgI, the data were fitted to a Gaussian for the early time part and an exponential for the longer time part. This procedure was used because it is known that the anisotropy should be Gaussian at very early times[24,34] and is further justified by the comparisons between the experiment and simulations discussed below. The fits yielded initial anisotropies of 0.05 for 320-nm excitation and 0.16 for 270-nm excitation, with half-widths of the Gaussian in the range 450−550 fs and exponential time constants of 8−10 ps.

Molecular Dynamics Simulations

Equilibrium molecular dynamics (MD) simulations were carried out to calculate the anisotropy of the diatomic HgI in ethanol (HgI/EtOH). The results from the MD simulations are used in the development of a microscopic interpretation of the product-state portion of the anisotropic transients measured through experiments. The dipole−dipole correlation function $\langle P_2[\mu(0)\cdot\mu(t)]\rangle$ is the relevant quantity obtained from the simulation where the dipole is along the molecular bond axis corresponding to the $^2\Sigma \rightarrow {}^2\Sigma$ transition of HgI. The details of the calculation, including the parameters and conditions, were previously reported.[53] Briefly, the simulated system consisted of an HgI molecule in 255 ethanol molecules with periodic boundary conditions using CHARMM.[54] The length of the box was ∼27 Å corresponding to the room-temperature density of ethanol. The HgI bond length was constrained at its equilibrium distance of 2.8 Å using SHAKE.[45] The results are the average of approximately 40 simulations that were run for 10 ps, with 0.5-fs time steps. The coordinates and velocities of HgI were saved every 5 fs. In addition, the angular momentum and rotational energy correlation functions were calculated to further elucidate the reorientational dynamics for the HgI/EtOH system.

The anisotropy calculated from the simulation is shown in Figure 2. A prominent feature is the sharp drop of the anisotropy from its maximum value at very early times. The shape at early times is reminiscent of the Gaussian decay that is expected for the anisotropy of an ensemble of freely rotating HgI molecules. A comparison of the free rotor correlation function with the simulated anisotropy is shown in Figure 2. The average rotational period estimated from a Gaussian fit of the fast part of the MD-simulated anisotropy was ca. 1.3 ps compared to ca. 1.5 ps for the free rotor. The appearance of the slower component of the anisotropy decay is interpreted to involve rotational diffusion dynamics. This longer time component of the simulated anisotropy decays with a time constant of ca. 6 ps. In the slip hydrodynamic limit,[55] the anisotropy

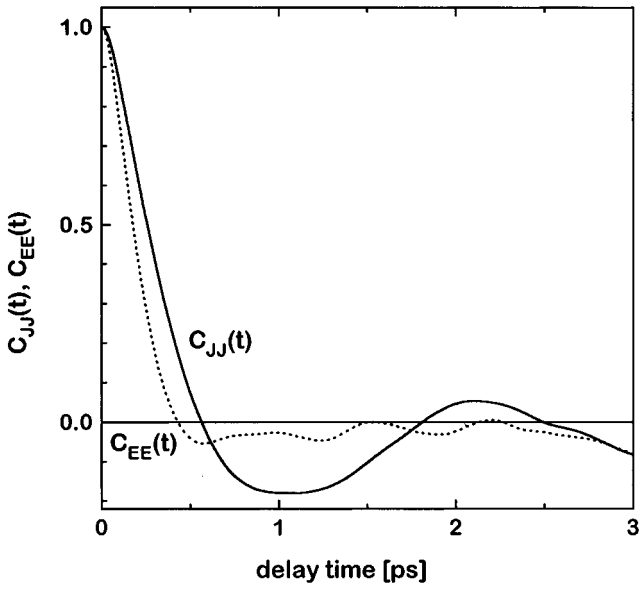

Figure 3. Normalized angular momentum correlation function $C_{JJ}(t)$ (solid line) and rotational kinetic energy correlation function $C_{EE}(t)$ (dotted line) calculated from the MD simulations.

decay time for HgI in ethanol is calculated to be ca. 2.2 ps, while the stick boundary conditions[56] yield 22.2 ps.

The normalized angular momentum correlation function, $C_{JJ}(t)$, shown in Figure 3 also provides additional information on the rotational dynamics. In the expression for $C_{JJ}(t)$,

$$C_{JJ}(t) = \frac{\langle \delta J(0) \cdot \delta J(t) \rangle}{\langle \delta J^2(0) \rangle} = \frac{\langle \delta \omega(0) \cdot \delta \omega(t) \rangle}{\langle \delta \omega^2(0) \rangle} \qquad (2)$$

δJ is the fluctuation of the angular momentum and $\delta\omega$ that of the angular velocity. It decays with a time constant of $\tau_J =$ 210 fs. The strong torques imparted by the surrounding solvent molecules seem to be capable of reversing the sense of HgI rotation as shown by the fact that $C_{JJ}(t)$ goes negative.[45] The damped oscillation can be interpreted as arising from the HgI molecules librating in the presence of the H-bonded solvent "cage", and collisions may be correlated for a short time period.[38,42] Also shown in Figure 3 is the rotational kinetic energy correlation function, $C_{EE}(t)$,

$$C_{EE}(t) = \frac{\langle \delta E(0) \delta E(t) \rangle}{\langle \delta E^2(0) \rangle} = \frac{\langle \delta J^2(0) \delta J^2(t) \rangle}{\langle \delta J^4(0) \rangle} \qquad (3)$$

where δE is the rotational energy fluctuation. C_{EE} decays with a time constant (τ_E) of ca.160 fs. This time corresponds to the decay of excess rotational energy assuming a linear response. The time scale of $C_{EE}(t)$ predicts that if there were a rotationally hot product distribution, the solvent will relax the excess rotational energy very quickly.

Discussion

Electronic States of HgI_2. First, we will discuss the nature of the transitions that could give rise to the observed anisotropies. Magnetic circular dichroism (MCD) data in hexane solution indicate that at 320 nm, mainly the $^1\Pi$ state of HgI_2 is pumped, whereas at 270 nm, the absorption also involves the $^1\Sigma^-$ state.[19] If indeed both states are pumped, the observed initial anisotropy of HgI is expected to be the combination of the respective canonical anisotropies listed in Table 1. In the following, it will be assumed that a $^2\Sigma \rightarrow {}^2\Sigma$ transition of HgI is probed, as is the case in the gas phase.[57−64] Furthermore, according to Table 1, if the probed transition of HgI were a $\Sigma \rightarrow \Pi$ transition, the anisotropy should never exceed 0.1, regardless of which HgI_2 transition were to be pumped, whereas an anisotropy of 0.16 was observed after excitation at 270 nm. From the initial anisotropy of 0.05 after excitation at 320 nm (determined by interpolation of the anisotropy data for HgI back to time zero assuming inertial dynamics, as described above), it can be concluded that the absorption of HgI_2 in ethanol at this wavelength must be composed of both $^1\Pi$ (58%) and $^1\Sigma^-$ (42%) contributions. At 270 nm, where an initial anisotropy of 0.16 is found, the contributions are changed to $^1\Pi$ (40%) and $^1\Sigma^-$ (60%). These numerical estimates assume the same yield of HgI following $^1\Pi$ or $^1\Sigma^-$ excitation by ignoring the symmetric stretch fragmentation into I + Hg + I. Fragmentation to this channel seems more likely when I is produced in its ground state I($^2P_{3/2}$) compared to I*($^2P_{1/2}$) with a spin−orbit splitting of 7600 cm^{-1}. Therefore, if the $^1\Pi$ excitation of HgI_2 were to generate mainly I($^2P_{3/2}$) and the $^1\Sigma^-$ excitation generated mainly I*($^2P_{1/2}$), as indicated by results on CdI_2,[65] then the ratio of the $^1\Pi$ to $^1\Sigma$ contributions to the absorption at each of the excitation wavelengths could be underestimated here.

Reactive Motion. The low initial anisotropy clearly arises because of the $^1\Pi$-state contribution to the probe transitions from the HgI_2 reactive potential. The fast rise of the anisotropy must therefore correspond to the reactive motion toward HgI in a $^2\Sigma$ state. In previous solution-phase work, HgI could be detected only after it had expanded to the attractive wall of the HgI potential well, which took about 120 fs.[15] As discussed above, the rise time of the anisotropy cannot be determined accurately from the present work but is on the order of 65 fs. This is consistent with the earlier work and could mean that the signal from the separating HgI and I fragments is freed from reactant excited-state ($^1\Pi$ or $^1\Sigma$) character after about one quarter of the vibrational period of either the asymmetric stretch motion of HgI_2 (65 fs) or of free HgI (60 fs). In practice, the time for an anisotropy signal to be freed from the characteristics of the reactant state can involve alterations in the frequency and nature of the probed transition, the relative absorption coefficients of the interconverting states, as well as the changing of the electronic wave functions associated with the dissociating states. Nevertheless, the time of 65 fs measured here represents one reasonable assessment of the lifetime of the transition state for this reaction.

Rotational Dynamics. After the reactive portion is completed, the anisotropy clearly exhibits a biphasic decay dominated by a faster part with a half-time of about 500 fs, followed by an exponential decay with a lifetime of 8−10 ps. This behavior is reminiscent of that exhibited by other diatomic molecules in solution as seen from the Raman line-shape analysis.[32−34,48,50] Examples of the rotational dynamics of diatomics measured in real time experiments are rare, but recently, Benjamin and co-workers[66] carried out simulations of the anisotropy decay of I_2^- generated from the I_3^- photodissociation which shows rotational dynamics[30,31] that are qualitatively similar to the results for HgI. In general, at the earliest times, the fast decay resembles the decay of the free rotor rotational coherence at the temperature of the solvent bath. At intermediate times, the decay deviates from that of the free rotor because the inertial motion soon becomes interrupted by solvent collisions, and changes in the magnitude and direction of the rotational angular momentum take place.[34]

A comparison of the equilibrium MD simulation of the HgI anisotropy decay and the experimental data is shown in Figure 4. Here, the simulation results were scaled to yield the same initial anisotropy $r(0)$ as the experiment, with the latter determined by a fit to the sum of a Gaussian and an exponential as described above. The apparent general agreement between

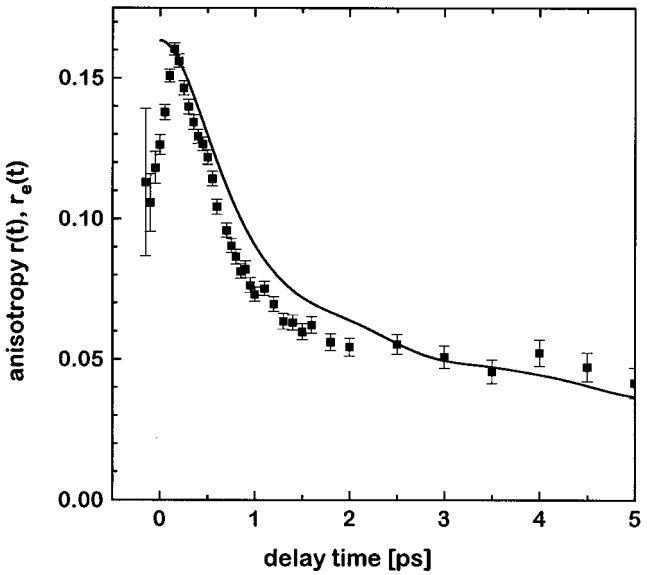

Figure 4. Comparison of the experimental and simulation results for the anisotropy decay. Shown are the anisotropy $r_e(t)$ observed with 270-nm pump, 490-nm probe and the result $r(t)$ of the MD simulations described in the text. The simulation results were scaled to yield the same initial anisotropy $r(0)$ as the experimental results, with $r_e(0)$ determined by a fit of the decaying part of $r_e(t)$ to the sum of a Gaussian and an exponential, as described in the text.

theory and experiment is very good. The lack of quantitative agreement between the experimental and simulation results might be due to the choice of interaction potential parameters between ethanol and HgI or to the neglect of the polarization effects in the simulation. The comparison of the free rotor correlation function with the early part of the calculated anisotropy decay, Figure 2, shows that free motion is dominating the calculated signal at the earliest times. Also, the portion of the calculated anisotropy decay up to 500 fs was shown to have an inertial component by noting that it was changed as expected for a free rotor when the moment of inertia of the molecule was increased or decreased by a factor of 2 by altering the masses. Simulations of this part of the anisotropy decay were the same when the HgI dipole was set to zero. The mass alterations did not significantly affect the slower portions of the calculated response which must be due to diffusion that depends on the molecular shape and volume and not on the masses. Removing the dipole of HgI did cause the slow part of the decay to speed up, consistent with the diffusive motion being determined by the strength of coupling to the surrounding solvent.

The simulations incorporate equilibrium conditions, while in the experiment the system is prepared impulsively and initially is known to have a nonequilibrium vibrational distribution.[15] It is of great interest to examine whether a nonequilibrium distribution of rotational excitations can be detected in a solution since this might allow the determination of the amount of energy deposited into rotations by a reaction. If the HgI were born rotationally hot, it should lose rotational coherence faster than predicted from the bath temperature until the rotational energy relaxation is completed. The relevant information is contained in the rotational energy correlation function shown in Figure 3, which decays in 160 fs. This result predicts that all the information about the initial distribution of rotational excitations is lost by 160 fs. The good agreement between the simulation and the experiment beyond 300 fs is certainly consistent with the system being rotationally equilibrated, although, in this case, the result is not surprising since the collinear dissociation of a nearly linear molecule into an atom and a diatom is unlikely to yield much rotational energy excess.[67]

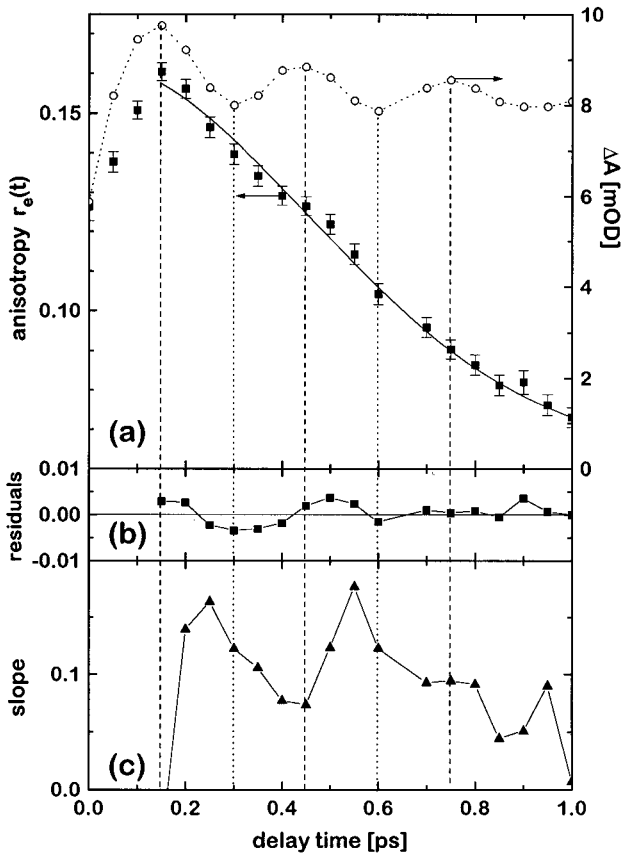

Figure 5. Oscillatory component in the HgI anisotropy decay. (a) Transient absorption (○, right axis) observed with magic angle polarization of pump and probe and anisotropy $r_e(t)$ (■, left axis) for 270-nm pump, 490-nm probe. The solid line corresponds to the best fit of the anisotropy decay after 150 fs to a sum of a Gaussian and an exponential. (b) Residuals of the fit. (c) Slope of the anisotropy decay, determined by calculating the instantaneous slope at each point from the data at the two neighboring points. The vertical lines indicate the delay times at which HgI is in its most extended (dashed lines) or most compressed (dotted lines) conformation and are drawn to indicate the correlation between the HgI motion and the oscillation in the anisotropy slope.

After the photodissociation, the excess translational energy of the diatomic fragment would be dumped into the surrounding solvent molecules during the initial collisions. This can heat the local solvent environment. In that case, the diffusional rotational dynamics observed may correspond to a higher than room temperature of the bath. However, we calculated the increase in temperature from dumping all the excess translational energy of the reaction into a volume of ethanol corresponding to the first solvation shell of HgI and found it to be negligible.

Vibrating Rotor Dynamics. It is evident from Figure 5, in particular from the residuals of the fits, that there is an oscillatory component on the early part of the anisotropy decay at 490 nm. These oscillations apparently correlate with the motion of the HgI wavepacket. The instantaneous slope of the experimental anisotropy decay function is plotted in Figure 5c, which makes clearer the origin of the oscillations: This slope is systematically lowest when the molecule is most extended, corresponding to the maxima of the transient absorption oscillations,[15,16] and largest when the molecule is compressed. In the time regime of the first 500 fs, the nature of the reorientation dynamics is not well defined, being neither inertial nor classically diffusive. As the wavepacket moves from the repulsive to the attractive side of the potential, both the moment of inertia and the hydrodynamic volume will increase and slow down the molecular reorientation. At the 490-nm probe wavelength, the observed HgI molecules at the center of the distribution are

stretching from about 2.65 to 3.2 Å.[15] The van der Waals length of HgI is 6.4 Å, as estimated from the sum of the bond length and the van der Waals radii of Hg and I. The van der Waals diameter of I is 4.3 Å so that the effective volume of HgI for hydrodynamic calculations is ca. 93 Å^3. The wavepacket motion will give rise to an 8.5% peak-to-peak oscillation in the molecular volume. Since the rotational diffusion time is generally proportional to volume,[23] this would result in an oscillation in the slope of the anisotropy decay of about the same magnitude if the motion were entirely diffusive. Such a modulation is somewhat smaller than but consistent with the experiment, given the signal to noise. There is also an inertial part to the modulation of the anisotropy, which is the time domain manifestation of the nonrigid rotor character of the HgI. We calculated the inertial rotational coherence decay of HgI treated as a free anharmonic nonrigid rotor and found oscillations in the slope of about the same magnitude as those that were estimated for diffusion. To the best of our knowledge, a wavepacket characteristic of this sort was not previously reported for a diffusing molecule. The analysis of a nonequilibrium simulation of vibrating HgI will assist in obtaining a fuller understanding of this effect and is expected to yield information about the spatial locations of the wavepacket, which is complementary to that obtained from transient absorption measurements.

Acknowledgment. This work was supported by the NSF-CHE and NIH. N.P. gratefully acknowledges the National Science Foundation for a postdoctoral fellowship in chemistry; M.V. gratefully acknowledges the Deutsche Forschungsgemeinschaft for a research fellowship.

References and Notes

(1) Wynne, K.; Hochstrasser, R. M. *Chem. Phys.* **1993**, *171*, 179.
(2) Hochstrasser, R. M.; Pereira, M. A.; Share, P. E.; Sarisky, M. J.; Kim, Y. R.; Repinec, S. T.; Sension, R. J. *Proc. Indian Acad. Sci.* **1991**, *103*, 351.
(3) Cross, A. J.; Waldeck, D. H.; Fleming, G. R. *J. Chem. Phys.* **1983**, *78*, 6455.
(4) Sension, R. J.; Repinec, S. T.; Szarka, A. Z.; Hochstrasser, R. M. *J. Chem. Phys.* **1993**, *98*, 6291.
(5) Kim, Y. R.; Share, P.; Pereira, M.; Sarisky, M.; Hochstrasser, R. M. *J. Chem. Phys.* **1989**, *91*, 7557.
(6) Zhu, F.; Galli, C.; Hochstrasser, R. M. *J. Chem. Phys.* **1993**, *98*, 1042−1057.
(7) Haran, G.; Wynne, K.; Moser, C. C.; Dutton, P. L.; Hochstrasser, R. M. *J. Phys. Chem.* **1996**, *100*, 5562.
(8) Raftery, D.; Sension, R. J.; Hochstrasser, R. M. In *Activated Barrier Crossing*; Fleming, G. R., Ed.; World Science: Singapore, 1993; p 163.
(9) Baumert, T.; Pedersen, S.; Zewail, A. H. *J. Phys. Chem.* **1993**, *97*, 12447.
(10) Pedersen, S.; Baumert, T.; Zewail, A. H. *J. Phys. Chem.* **1993**, *97*, 12460.
(11) Gruebele, M.; Roberts, G.; Zewail, A. H. *Philos. Trans. R. Soc. London, Ser. A* **1990**, *332*, 223.
(12) Dantus, M.; Bowman, R. M.; Gruebele, M.; Zewail, A. H. *J. Chem. Phys.* **1989**, *91*, 7437.
(13) Bowman, R. M.; Dantus, M.; Zewail, A. H. *Chem. Phys. Lett.* **1989**, *156*, 131.
(14) Dantus, M.; Bowman, R. M.; Baskin, J. S.; Zewail, A. H. *Chem. Phys. Lett.* **1989**, *159*, 406.
(15) Pugliano, N.; Szarka, A. Z.; Hochstrasser, R. M. *J. Chem. Phys.* **1996**, *104*, 5062.
(16) Pugliano, N.; Szarka, A. Z.; Gnanakaran, S.; Treichel, M.; Hochstrasser, R. M. *J. Chem. Phys.* **1995**, *103*, 6498.
(17) Pugliano, N.; Szarka, A. Z.; Palit, D. K.; Hochstrasser, R. M. *J. Chem. Phys.* **1993**, *99*, 7273.
(18) Maya, J. *J. Chem. Phys.* **1977**, *67*, 4967.
(19) Savas, M. M.; Mason, W. R. *Inorg. Chem.* **1988**, *27*, 658.
(20) Hoffman, H.; Leone, S. R. *J. Chem. Phys.* **1978**, *69*, 3819.
(21) Wynne, K.; Hochstrasser, R. M. *J. Raman Spectros.* **1995**, *26*, 561.
(22) Burshtein, A. I.; Temkin, S. I. *Spectroscopy of Molecular Rotation in Gases and Liquids*; Cambridge University: Cambridge, 1994.
(23) Berne, B. J.; Pecora, R. *Dynamic Light Scattering*; Wiley: New York, 1976.
(24) Steele, W. A.; Streett, W. B. *Mol. Phys.* **1980**, *39*, 279.
(25) Gordon, R. G. *Adv. Mag. Reson.* **1965**, *3*, 1.
(26) Steele, W. A. In *Transport Phenomena in Fluids*; Hanley, H. J. M., Ed.; Dekker: New York, 1969; p Chapter 8.
(27) Evans, M. W.; Evans, G. J.; Coffey, W. T.; Grigolini, P. *Molecular Dynamics*; Wiley: New York, 1982.
(28) Perchard, J. P.; Murphy, W. F.; Bernstein, H. J. *Mol. Phys.* **1972**, *23*.
(29) Ishol, L. M.; Scott, T. A.; Goldblatt, M. *J. Mag. Reson.* **1976**, *23*, 313.
(30) Banin, U.; Kosloff, R.; Ruhman, S. *Isr. J. Chem.* **1993**, *33*, 141.
(31) Banin, U.; Ruhman, S. *J. Chem. Phys.* **1993**, *98*, 4391.
(32) Gordon, R. G. *J. Chem. Phys.* **1965**, *42*, 3658.
(33) Gordon, R. G. *J. Chem. Phys.* **1965**, *43*, 1307.
(34) Gordon, R. G. *J. Chem. Phys.* **1966**, *44*, 1830.
(35) Debye, P. *Polar Molecules*; Dover: New York, 1928.
(36) Steele, W. A. *J. Chem. Phys.* **1963**, *38*, 2404.
(37) Steele, W. A. *J. Chem. Phys.* **1963**, *38*, 2411.
(38) Lindenberg, K.; Cukier, R. I. *J. Chem. Phys.* **1975**, *62*, 3271.
(39) Fixman, M.; Rider, K. *J. Chem. Phys.* **1969**, *51*, 2425.
(40) Chandler, D. *J. Chem. Phys.* **1974**, *60*, 1974.
(41) Ivanov, E. N. *JETP* **1964**, *18*, 1041.
(42) Lynden-Bell, R. M.; Steele, W. A. *J. Phys. Chem.* **1984**, *88*, 6514.
(43) Lynden-Bell, R. M.; McDonald, I. R. *Chem. Phys. Lett.* **1982**, *89*, 105.
(44) Kievlson, D.; Keyes, T. *J. Chem. Phys.* **1972**, *57*, 4599.
(45) Allen, M. P.; Tildesley, D. J. *Computer Simulation of Liquids*; Clarendon: Oxford, 1987.
(46) Berne, B. J.; Harp, G. D. *Adv. Chem. Phys.* **1970**, *17*, 63.
(47) Kabadi, V. N.; Steele, W. A. *J. Phys. Chem.* **1985**, *89*, 1467.
(48) Temkin, S. I.; Steele, W. A. *Chem. Phys. Lett.* **1993**, *215*, 285.
(49) Frenkel, D.; McTague, J. P. *J. Chem. Phys.* **1980**, *72*, 2801.
(50) Steele, W. A. *J. Mol. Liq.* **1991**, *48*, 321.
(51) Barojas, J.; Levesque, D.; Quentrec, B. *Phys. Rev. A* **1973**, *7*, 1092.
(52) Wynne, K.; Reid, G. D.; Hochstrasser, R. M. *Opt. Lett.* **1994**, *19*, 895.
(53) Gnanakaran, S.; Hochstrasser, R. M. *J. Chem. Phys.* **1996**, *105*, 3486.
(54) Brooks, B. R.; Bruccoleri, R. E.; Olafson, B. D.; States, D. J.; Swaminathan, S.; Karplus, M. *J. Comp. Chem.* **1983**, *4*, 187.
(55) Sension, R. J.; Hochstrasser, R. M. *J. Chem. Phys.* **1993**, *98*, 2490.
(56) Barkley, M. D.; Kowalczyk, A. A.; Brand, L. *J. Chem. Phys.* **1981**, *75*, 3581.
(57) Jordon, K. J.; Bascal, H. A.; Lipson, R. H.; Melchoir, M. *J. Mol. Spectrosc.* **1993**, *159*, 144.
(58) Lipson, K. J.; Lipson, R. Z.; Yang, D. S. *J. Chem. Phys.* **1992**, *97*, 9099.
(59) Jordon, K. J.; Lipson, R. H.; McDonald, N. A.; LeRoy, R. J. *J. Phys. Chem.* **1992**, *96*, 4778.
(60) Zhang, F. M.; Oba, D.; Sester, D. W. *J. Phys. Chem.* **1987**, *91*.
(61) Dreiling, T. D.; Setser, D. W. *J. Chem. Phys.* **1983**, *79*, 5423.
(62) Viswanathan, K. S.; Tellinghuisen, J. *J. Mol. Spectros.* **1983**, *98*, 185.
(63) McGarvey, J. A.; Cheung, N.; Erlandson, A. C.; Cool, T. A. *J. Chem. Phys.* **1981**, *74*, 5133.
(64) Cheung, N.; Cool, T. A. *Quantum Spectrosc. Radiat. Transfer* **1979**, *21*, 397.
(65) Kawasaki, K.; Lee, S. J.; Bersohn, R. *J. Chem. Phys.* **1979**, *71*, 1235.
(66) Benjamin, I. *J. Chem. Phys.* **1993**, *98*, 8337.
(67) Levine, R. D.; Bernstein, R. B. *Molecular Reaction Dynamics and Chemical Reactivity*; Oxford University: New York, 1987.